



# UNIVERSITÀ DI PARMA

## ARCHIVIO DELLA RICERCA

University of Parma Research Repository

$\epsilon$ -Ga 2 O 3 epilayers as a material for solar-blind UV photodetectors

This is the peer reviewed version of the following article:

*Original*

$\epsilon$ -Ga 2 O 3 epilayers as a material for solar-blind UV photodetectors / Pavesi, M.; Fabbri, F.; Boschi, F.; Piacentini, Giovanni; Baraldi, A.; Bosi, M.; Gombia, E.; Parisini, A.; Fornari, R.. - In: MATERIALS CHEMISTRY AND PHYSICS. - ISSN 0254-0584. - 205:(2018), pp. 502-507. [10.1016/j.matchemphys.2017.11.023]

*Availability:*

This version is available at: 11381/2837963 since: 2021-10-13T11:51:47Z

*Publisher:*

Elsevier Ltd

*Published*

DOI:10.1016/j.matchemphys.2017.11.023

*Terms of use:*

Anyone can freely access the full text of works made available as "Open Access". Works made available

*Publisher copyright*

note finali coverpage

(Article begins on next page)

02 May 2026

Chemistry and Physics

Elsevier Editorial System(tm) for Materials

Manuscript Draft

Manuscript Number: MATCHEMPHYS-D-17-00272R2

Title:  $\epsilon$ -Ga<sub>2</sub>O<sub>3</sub> epilayers as a material for solar-blind UV photodetectors

Article Type: Full Length Article

Keywords: solar-blind UV detectors, gallium oxide, thin films, epsilon phase, photoconductivity.

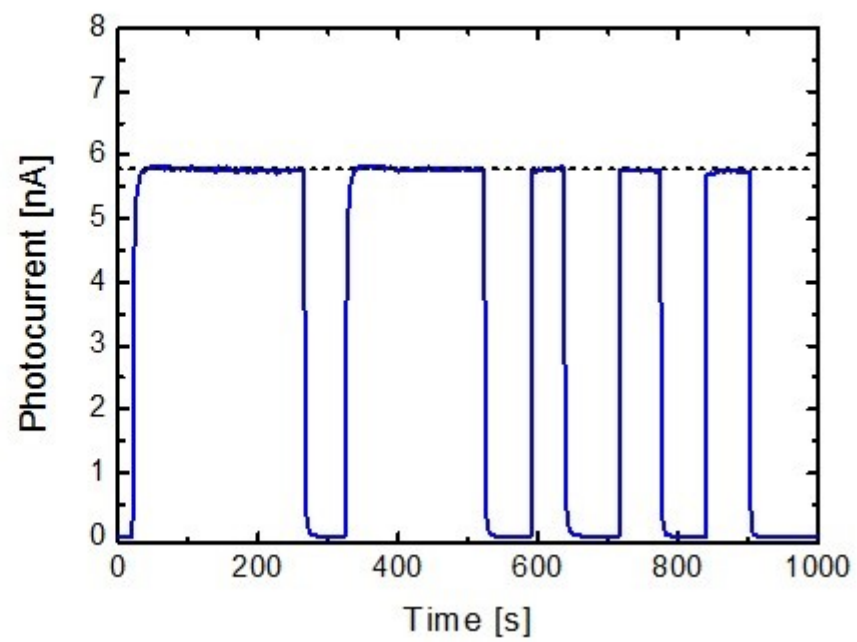
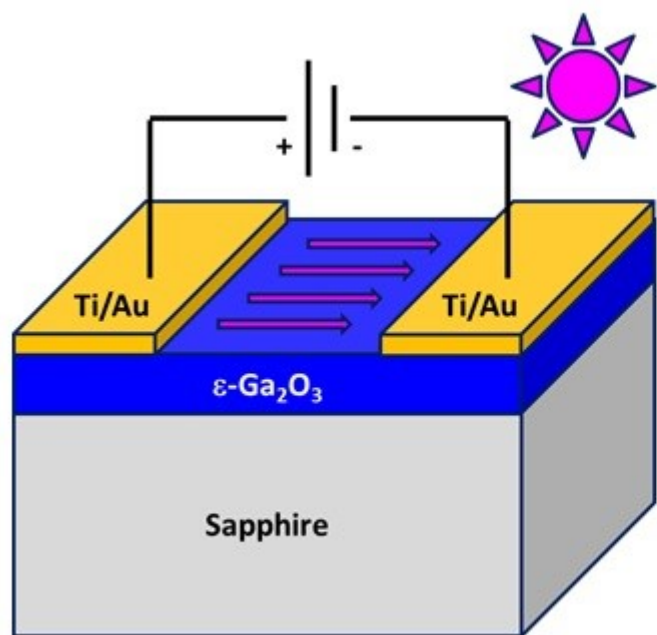
Corresponding Author: Dr. Maura Pavesi, PhD

Corresponding Author's Institution: University of Parma

First Author: Maura Pavesi, PhD

Order of Authors: Maura Pavesi, PhD; Filippo Fabbri, Ph.D.; Francesco Boschi, Ph.D.; Giovanni Piacentini, Ph.D.; Andrea Baraldi, Prof.; Matteo Bosi, Ph.D.; Enos Gombia, Dr.; Antonella Parisini, Prof.; Roberto Fornari, Prof.

Abstract: Electrical and optical properties of undoped single-phase  $\epsilon$ -Ga<sub>2</sub>O<sub>3</sub> epitaxial films prepared by MOCVD are reported. It is shown that this still unexplored polymorph of gallium oxide possesses wide bandgap and very high dark resistivity, thus allowing the design and fabrication of solar-blind UV photodetectors. Simple cost-effective photoresistors, fabricated by direct deposition of the epilayers on c-oriented sapphire substrates, exhibited good performance. The physical properties and the photoresponse of  $\epsilon$ -Ga<sub>2</sub>O<sub>3</sub> make this material very interesting in view of novel applications.



## Highlights

- Epilayers of  $\epsilon$ -Ga<sub>2</sub>O<sub>3</sub> are employed for the first time as UV photodetectors.
- Fabricated photoresistors are sensitive to UV (270 nm), stable and reliable.
- Their properties compare well with those of the  $\beta$  polytype of Ga<sub>2</sub>O<sub>3</sub>.
- Bandgap and deep levels are investigated by optical absorption/cathodoluminescence.

## $\epsilon$ -Ga<sub>2</sub>O<sub>3</sub> epilayers as a material for solar-blind UV photodetectors

1  
2  
3  
4  
5  
6 M. Pavesi <sup>a,b,\*</sup>, F. Fabbri <sup>b,c</sup>, F. Boschi <sup>a,b</sup>, G. Piacentini <sup>a</sup>, A. Baraldi <sup>a</sup>, M. Bosi <sup>b</sup>, E. Gombia <sup>b</sup>, A.  
7 Parisini <sup>a,b</sup>, and R. Fornari <sup>a,b</sup>  
8  
9

10  
11  
12  
13  
14 <sup>a</sup> *Dept. of Mathematical, Physical and Computer Sciences, Univ. of Parma, Parco Area delle*  
15 *Scienze 7/A, 43124 Parma, Italy*  
16

17  
18 <sup>b</sup> *IMEM-CNR Institute of Materials for Electronics and Magnetism, Parco Area delle Scienze 37/A,*  
19 *43124 Parma, Italy*  
20  
21

22  
23 <sup>c</sup> *Center for Nanotechnology Innovation @NEST, Istituto Italiano di Tecnologia, Piazza San*  
24 *Silvestro 12, 56127 Pisa, Italy*  
25  
26

27  
28  
29  
30  
31 \*Corresponding author

32  
33 E-mail address: [maura.pavesi@unipr.it](mailto:maura.pavesi@unipr.it)  
34

35  
36 Address: Dept. of Mathematical, Physical and Computer Sciences, Univ. of Parma, Parco Area  
37  
38 delle Scienze 7/A, 43124 Parma, Italy  
39

40  
41  
42  
43 **Keywords:** solar-blind UV detectors, gallium oxide, thin films, epsilon phase, photoconductivity  
44  
45  
46  
47  
48  
49  
50  
51  
52  
53  
54  
55  
56  
57  
58  
59  
60  
61  
62

## Abstract

Electrical and optical properties of undoped single-phase  $\epsilon$ -Ga<sub>2</sub>O<sub>3</sub> epitaxial films prepared by MOCVD are reported. It is shown that this still unexplored polymorph of gallium oxide possesses wide bandgap and very high dark resistivity, thus allowing the design and fabrication of solar-blind UV photodetectors. Simple cost-effective photoresistors, fabricated by direct deposition of the epilayers on *c*-oriented sapphire substrates, exhibited good performance. The physical properties and the photoresponse of  $\epsilon$ -Ga<sub>2</sub>O<sub>3</sub> make this material very interesting in view of novel applications.

## 1. Introduction

Oxides are materials with very high potential for novel generations of electronic devices, especially for sensing and energy applications. Among the oxide compounds, sesquioxides (In<sub>2</sub>O<sub>3</sub>, Ga<sub>2</sub>O<sub>3</sub>, Al<sub>2</sub>O<sub>3</sub>, and their ternary alloys) have attracted much attention as they present a wide band gap that ranges from 3.7 eV for In<sub>2</sub>O<sub>3</sub> to 8.9 eV for Al<sub>2</sub>O<sub>3</sub>, and lend themselves for many applications, such as power diodes and transistors, gas sensors, and UV photodetectors. Most technological and scientific research activities have so far been focused on  $\beta$ -Ga<sub>2</sub>O<sub>3</sub> [1, 2] (monoclinic lattice), as it is the thermodynamically stable polymorph and easy to prepare in form of single crystals [3], thin epilayers [4], and nanostructures [5]. However,  $\beta$ -Ga<sub>2</sub>O<sub>3</sub> generally presents anisotropic physical properties, and the single crystals are known to be prone to cleavage, which of course poses serious problems at the time of device manufacturing. For these reasons, there is a growing interest also on metastable polytypes, where metastable means that they tend to convert to  $\beta$  phase upon high-temperature annealing. These polytypes present a crystallographic structure of much higher symmetry (cubic or hexagonal) and are appealing since they do not exhibit the anisotropy typical of the  $\beta$  phase.

Recent work of some of the present the authors on heteroepitaxial growth of Ga<sub>2</sub>O<sub>3</sub> demonstrated the coherent growth of  $\epsilon$ -Ga<sub>2</sub>O<sub>3</sub> on sapphire [6]. This polytype was seen to be stable when

1 thermally annealed in oxygen atmosphere up to 700 °C, thus allowing the fabrication of devices that  
2 work at room or higher temperature. The availability of a hexagonal phase of Ga<sub>2</sub>O<sub>3</sub>, with good  
3 crystallographic matching to gallium and aluminum nitride, and stable up to relatively high  
4 temperatures, is also intriguing in view of developing novel nitride-based devices. Indeed, they may  
5 take advantage of the more favorable symmetry and epitaxial relationships with respect to the  
6 monoclinic phase.  
7

8 The  $\epsilon$ -phase was first observed in the middle of the last century in  $\beta$ -contaminated precipitates that  
9 had resulted from thermal decomposition of Ga(NO<sub>3</sub>)<sub>3</sub> [7], and a recent study showed that this  
10 phase belongs to the high symmetry hexagonal system with space group  $P6_3mc$  [8]. The study was  
11 however carried out on samples that contained more phases than pure  $\epsilon$ , which obviously poses  
12 some limits to the accuracy of lattice parameter determination.  
13

14 Single-phase  $\epsilon$ -Ga<sub>2</sub>O<sub>3</sub> layers were obtained for the first time by Oshima *et al.* by halide vapor phase  
15 epitaxy (HVPE) on GaN, AlN, and  $\beta$ -Ga<sub>2</sub>O<sub>3</sub> substrates [9], and a little later by Boschi *et al.* [6] and  
16 Xia *et al.* [10] by means of Metal Organic Chemical Vapour Deposition (MOCVD), respectively on  
17 c-oriented sapphire and 6H-SiC.  
18

19 Unfortunately, a detailed analysis of the  $\epsilon$ -Ga<sub>2</sub>O<sub>3</sub> physical properties and of its potential use in  
20 devices is still lacking, which is the principal motivation of the present paper. Here, we shall first  
21 report on the results of optical and electrical investigations of  $\epsilon$ -Ga<sub>2</sub>O<sub>3</sub> films on c-oriented sapphire,  
22 and then show an application of this material as photo-detector for deep-UV radiation. The  
23 produced devices demonstrated very good performance in terms of photoresponse, stability, and  
24 reproducibility. The UV-response is adequately fast and reliable to render this “unusual” Ga<sub>2</sub>O<sub>3</sub>  
25 phase a subject of great interest for future applications.  
26

## 27 **2. Electro-optical investigation and photodetector characteristics**

28 The samples studied and processed in this work were grown by MOCVD on c-oriented 2-inches  
29 sapphire substrates heated at 650 °C under the growth conditions reported in detail in ref. [6].  
30

Trimethylgallium (TMG) and ultrapure water, stored in dedicated stainless steel bubblers kept at 2 °C and 30 °C, respectively, were employed as precursors. The ratio of the reagent partial pressures in the growth chamber ( $p_{\text{H}_2\text{O}} / p_{\text{TMG}}$ ) was  $>1000$ . The films were transparent and smooth, as checked by SEM (see Fig 1). Previous XRD and AFM investigations, reported in ref. [6], on the same films used for the present work, confirm that they are single-phase  $\epsilon\text{-Ga}_2\text{O}_3$  and present a maximum roughness of  $\pm 3$  nm, although the typical roughness RMS is 1.5 nm. A later investigation by X-ray and high-resolution TEM, performed on our high-quality epilayers, showed that the hexagonal  $\epsilon$  phase actually consists of ordered  $120^\circ$ -rotational twin domains 5-10 nm in size. These nano-domains have an orthorhombic structure with  $Pna21$  space group symmetry, the so-called  $\kappa\text{-Ga}_2\text{O}_3$  [11].

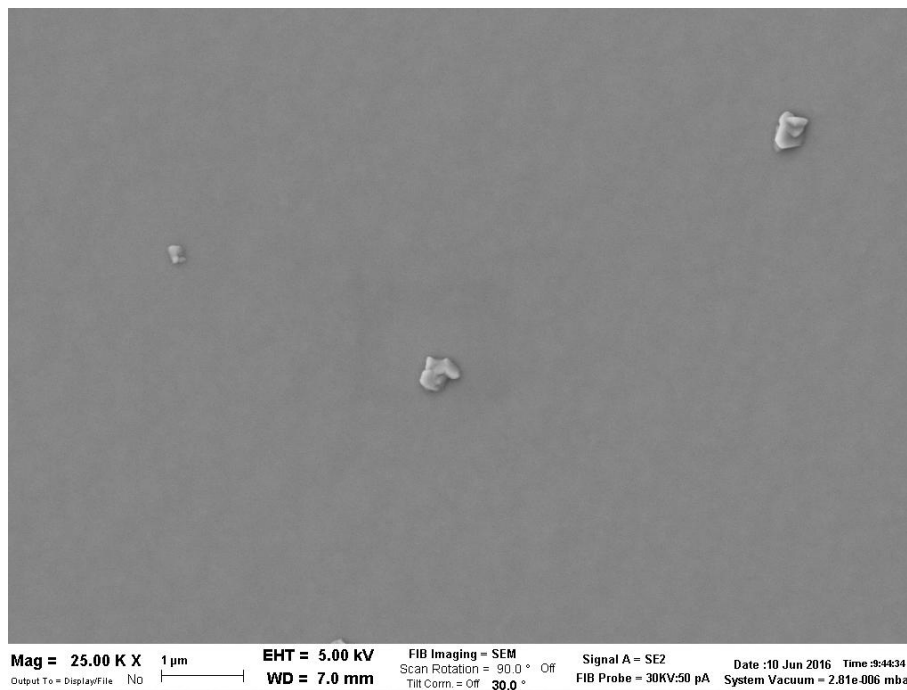


Fig. 1: SEM image for a representative  $\epsilon\text{-Ga}_2\text{O}_3$  film.

One-face planar-geometry metal–semiconductor–metal was employed for electro-optical characterization. The electrodes, consisting of Au (250 nm) / Ti (20 nm) bilayer, were deposited through a metal mask by thermal evaporation, followed by 10 minutes annealing at 500 °C. The reproducibility of the Au/Ti contact deposition was verified on a large number of thin films,

confirming the robustness of the fabrication procedure. Typically, thin film large-area photodetectors, with a distance of 2 mm between electrodes, were fabricated and measured in this study. As shown below, electrodes were ohmic over the wide range of applied biases and very stable in time and after several temperature cycles.

The photoresponse of  $\epsilon$ -Ga<sub>2</sub>O<sub>3</sub> thin films was studied in air at fixed temperature (25°C) and constant humidity. The experimental apparatus for Photocurrent Spectroscopy (PCS) consisted of a light source system ORIEL Mod. 66882 suitably screened and focused with an ORIEL Xenon – 300 W lamp, neutral filters, a monochromator CornerStone 130TM 1/8 m Mod. 74000 covering the range 200 ÷ 1600 nm (wavelength resolution of 3 nm). The chopped monochromatic light was focused on the free surface of the  $\epsilon$ -Ga<sub>2</sub>O<sub>3</sub> film between two Au/Ti electrodes. The spectral distribution of the light beam was measured using a Hamamatsu Photonic Multi-Channel Analyzer PMA-11 and a correction factor was introduced for all the measured spectra, taking into account the spectral distortion of metal contacts, measured for a reference Au/Ti layer of the same thickness deposited on quartz.

The mean irradiance on the active surface of sample detectors (i.e. outside the metal contacts) in the spectral region 200 ÷ 400 nm was around 1 mW cm<sup>-2</sup>. The photon flux was varied intercepting the light beam with optical neutral filters having optical density in the range 0.1 ÷ 8.0. Voltages between 0 and 200 V were applied to the contacts by means of a Source-Meter Keithley Mod. 2400. Measurements of the dark current at a function of temperature in the range 20-300°C showed that the film conductance increases by three orders of magnitude with the temperature. The corresponding Arrhenius plot is linear and presents an activation energy of 0.695 eV (Fig. 2). This effect is possibly related to the thermal ionization of relatively deep electronic levels located at about 0.7 eV below the conduction band. Similar electronic states were previously detected by DLTS in  $\beta$ -Ga<sub>2</sub>O<sub>3</sub> single crystals [12], although their nature was not clarified.

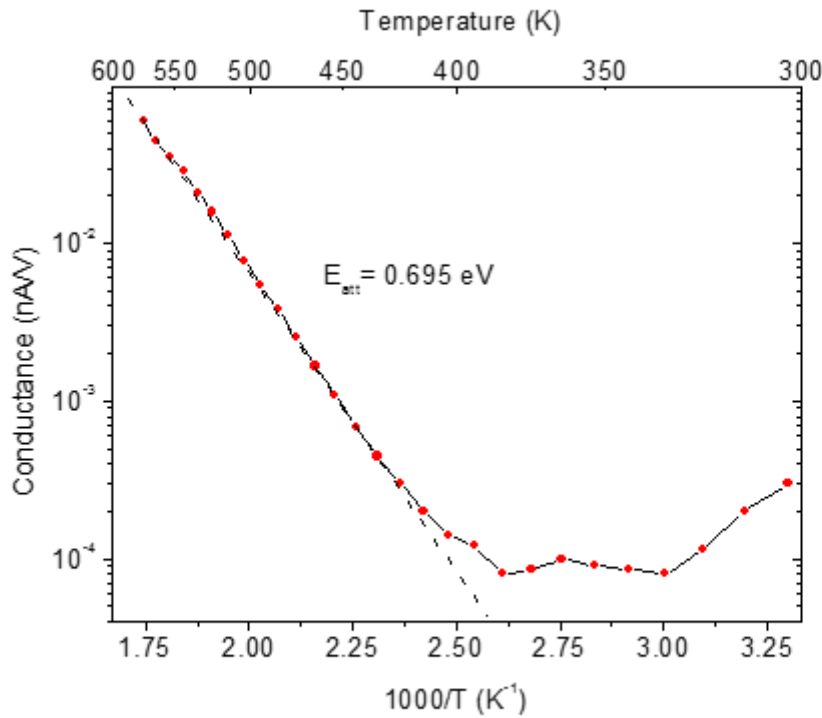


**Fig. 2:** Arrhenius plot for the dark current in the temperature range 20 ÷ 300 °C.

The photoconductivity spectrum (PCS) for a representative thin film detector is shown in Fig. 3, along with the corresponding optical absorption spectrum. All investigated samples practically showed the same behavior.

Let us examine some aspects of the photocurrent and absorption spectra shown in Fig. 3: though similar, they present some remarkable differences. This can however be explained by considering that photocurrent depends on the concentration and lifetime of photo-carriers, i.e. on the number of photogenerated carriers that actually reach the electrodes. These two entities are not independent of each other, as, for instance, a higher concentration of traps can actually produce more photo-carriers, but also shorten their lifetime; it is the competition between coexisting phenomena that ultimately determines how many carriers do reach the electrodes.

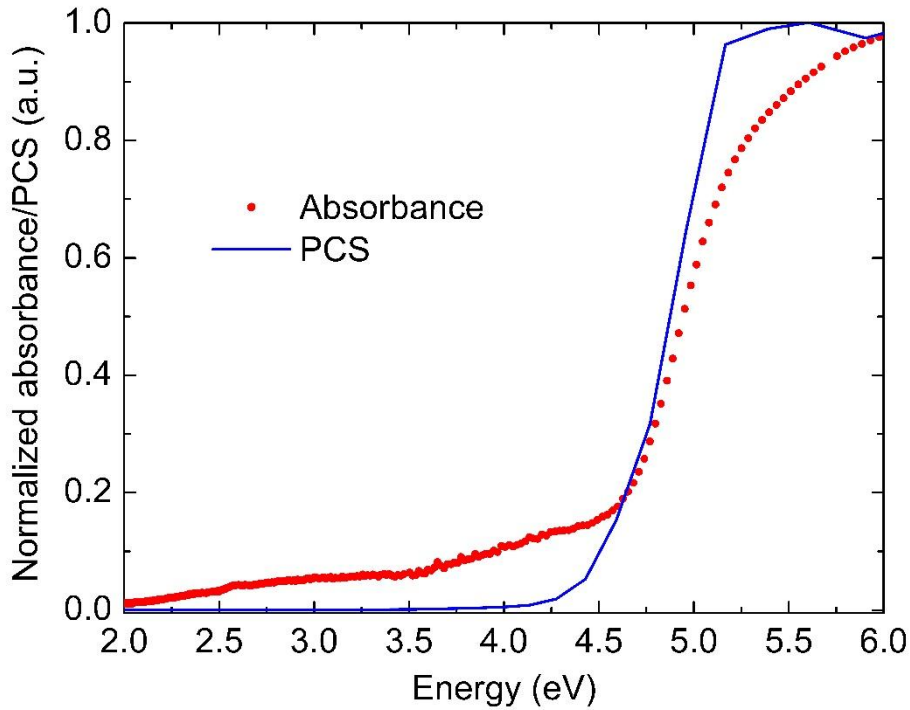


**Fig. 3:** Spectral photocurrent and optical absorption edge (normalized curves).

The normalized PCS curve of Fig. 3 shows a relatively mild onset at about 4.2 eV that becomes much sharper at about 4.6 eV. The onset of photoconductivity occurs below the estimated bandgap and is ascribed to the presence of energy levels connected with point defects or complexes, as already observed for  $\beta$ -Ga<sub>2</sub>O<sub>3</sub> [13, 14]. The optical absorption spectra, recorded at room temperature by using a Varian 2390 spectrophotometer and a 500  $\mu$ m thick sapphire substrate as reference, look somewhat different: a non-negligible absorption is present already at 2 eV, and it increases monotonically up to band edge. The long tail, extending from the absorption edge down to 2.1 eV, may include other components in addition to excitation of photocarriers from deep levels, for example light absorption by defects at substrate/film interface, etc. Photocurrent values in the same spectral region, far from bandgap edge, are too low to be appreciable in the same linear plot of Fig. 3. It is to be noted that the photogenerated current is low even when the absorbance is non-negligible.

1 Considering that the bandgap width is a most crucial parameter in order to define the working range  
2 of a semiconductor photodetector, we made an assessment of the bandgap of  $\varepsilon$ -Ga<sub>2</sub>O<sub>3</sub> by carrying  
3 out absorbance measurements on a large set of films with thicknesses in the range 175 nm ÷ 2  $\mu$ m.  
4 In all cases, the onset due to band-band absorption started at about 4.6 eV and the measured  
5 absorption coefficients were in good agreement with those extrapolated from the data of Oshima *et*  
6 *al* [9]. However, attempts to apply the standard Tauc plot ( $(\alpha h\nu)^2$  vs.  $h\nu$ ) for the analysis of the  
7 experimental absorbance failed, as the extrapolated absorption edges changed with the layer  
8 thickness, i.e. the thinner the layer the higher its apparent bandgap. Furthermore, they all shifted  
9 above 5 eV. Obviously, this fact cannot have a physical meaning, since the energy gap of a given  
10 material is an intrinsic property and it may not depend on the specimen geometry.

11 The impossibility of finding a unique bandgap from the Tauc plots suggests that some precaution  
12 has to be taken when dealing with absorption in very thin films, as previously pointed out for  
13 amorphous silicon [15]. It also indicates that an extended theoretical and experimental investigation  
14 on the band structure of this polytype is needed, aimed at clarifying if the band is direct or indirect.  
15 Nevertheless, for the purpose of the present work, we succeed to reconcile the experimental  
16 absorbance of  $\varepsilon$ -Ga<sub>2</sub>O<sub>3</sub> layers of variable thickness by simply analyzing the absorption coefficients  
17 as a function of photon energy. This analysis, based on the set of films with thickness between 175  
18 nm and 2  $\mu$ m, showed that the optical bandgap of all tested  $\varepsilon$ -Ga<sub>2</sub>O<sub>3</sub> films converges between 4.6  
19 eV and 4.7 eV, hence not so different from that observed for  $\beta$ -Ga<sub>2</sub>O<sub>3</sub> [16, 17].

20 The current-voltage curves, carried out in dark and under illumination at different wavelength, are  
21 shown in Fig. 4 and confirm a linear behavior over a wide range of applied biases. Remarkably,  
22 Au/Ti contacts were easily fabricated, with good ohmic characteristics. The good linearity of  
23 contacts was verified for temperatures up to 300 °C and for incoming light intensities at 250 nm up  
24 to about 1.8 mW/cm<sup>2</sup> (inset of Fig. 4).

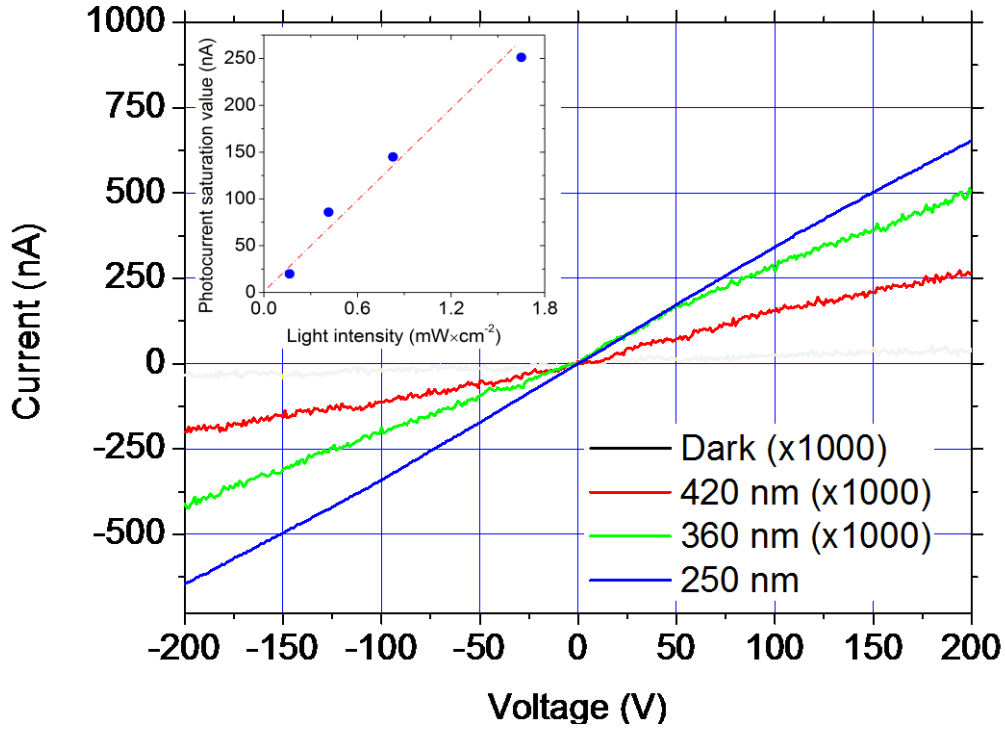


**Fig. 4:** current-voltage curves in dark and under illumination at different wavelengths. Inset: photocurrent saturation values at fixed applied voltage (75V) as a function of the light intensity (250 nm).

The performance of the  $\epsilon$ -Ga<sub>2</sub>O<sub>3</sub> UV detector is shown in Fig. 5. The photogenerated signal shows good stability over a long time (a few hundred seconds). After multiple on/off illumination cycles, the photodetector maintained an identical response, demonstrating robustness and good reproducibility. The noise affecting the current output under illumination was estimated to be well below 1%.

The photocurrent transients for on/off operations was also analyzed: the transient following the switch-on may be well described by a single exponential with time constant of 2.5 s, whereas the switch-off shows a bi-exponential behavior ( $\tau_1 = 0.4$ s and  $\tau_2 = 2.6$ s, inset of Fig. 5). Photocurrent reaches saturation over longer times (typically few tens of seconds), but with a behavior that depends on the previous illumination of the sample (see repeated on/off in Fig. 5) and on the wavelength of incident photons.

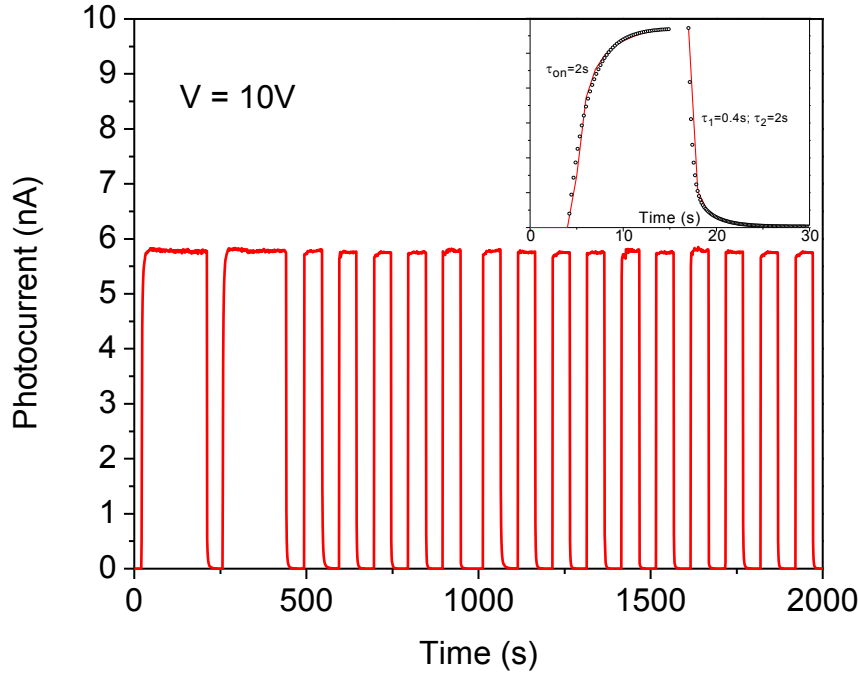


**Fig. 5:** Time-dependent photoresponse to UV light (270 nm) under an applied bias voltage ( $V = 10V$ ). Switching on/off with different intervals of time confirms a good stability even over long times. Inset: best fit for the switching on ( $\tau_{on} \sim 2$  s) and off ( $\tau_1 \sim 0.4$  s and  $\tau_2 \sim 2$  s, see text for details).

This behavior, already reported by other authors [5,18], could be ascribed to surface states that strongly influence the photocurrent process, and that obviously modify their action according to penetration depth and intensity of incoming light, as well as (previous) ionization status of the levels. All these features, in particular the difference of photocurrent for illumination below/above bandgap of about three orders of magnitude (Fig. 4), make  $\epsilon\text{-Ga}_2\text{O}_3$  a very promising material for solar-blind detector applications. Its photo-responsivity indeed compares well with that of  $\beta\text{-Ga}_2\text{O}_3$ , a proven material for deep-UV detection [2, 18, 19].

In order to check the distribution of deep electronic states as a function of the film thickness, in particular when approaching the film surface and substrate/film interface, we performed some cathodo-luminescence spectroscopy measurements by means of a commercial Gatan monoCL system, mounted onto an S360 Cambridge Scanning Electron Microscope. The system was

equipped with grating and a multi-alkali photomultiplier sensitive in the range 350 ÷ 830 nm (3.6 ÷ 1.5 eV). The spectra were collected with a constant power density.

In Fig. 6a we reported the CL spectra for a representative  $\epsilon$ -Ga<sub>2</sub>O<sub>3</sub> film as a function of three different accelerating voltage, i.e. electron penetration depth of 50, 150 and 460 nm. The measurements were repeated on different samples to assess the reproducibility of the growth results. The Gaussian deconvolution of the spectra provides three broad bands centered at 2.34 eV (530 nm), 2.67 eV (464 nm), and 2.75 eV (450 nm), respectively (see inset of Fig. 6a, for the spectrum corresponding to penetration of 460 nm). With the same bands, but with different specific intensities, it was possible to fit other spectra as well. No band-band emission was detected, which is common also for other Ga<sub>2</sub>O<sub>3</sub> polymorphs.

The CL spectra were deconvoluted using a standard Levenberg-Marquardt algorithm to minimize the Chi-Square. To avoid any possible artifacts, we applied constraint on only the full width at half maximum (w) and set the peak position (xC) and amplitude (A) as free fitting parameters. We imposed a w maximum equal to 0.5 eV. As a result of the fitting, all peak positions were affected by an error of 0.01 eV, lower than the error from the spectral resolution of the system (5 nm). The uncertainty in A and w determination was estimated to be about 5%. The origin of these emission bands is not known yet, but the comparison with literature data for the more studied  $\beta$ -Ga<sub>2</sub>O<sub>3</sub> suggests that the three main bands could be connected with intra-gap donor-acceptor pairs due to point defects [20, 21].

As mentioned above, the electron penetration depth was varied between 50 to 450 nm by varying the accelerating voltage between 2.5 and 10 keV. This allowed a depth-resolved CL analysis and the study of the radiative centers distribution along the film cross-section, as previously made for other materials [22]. The volumes affected by generation and recombination mechanisms at different accelerating voltage were estimated from Montecarlo simulations performed with the CASINO software [23].

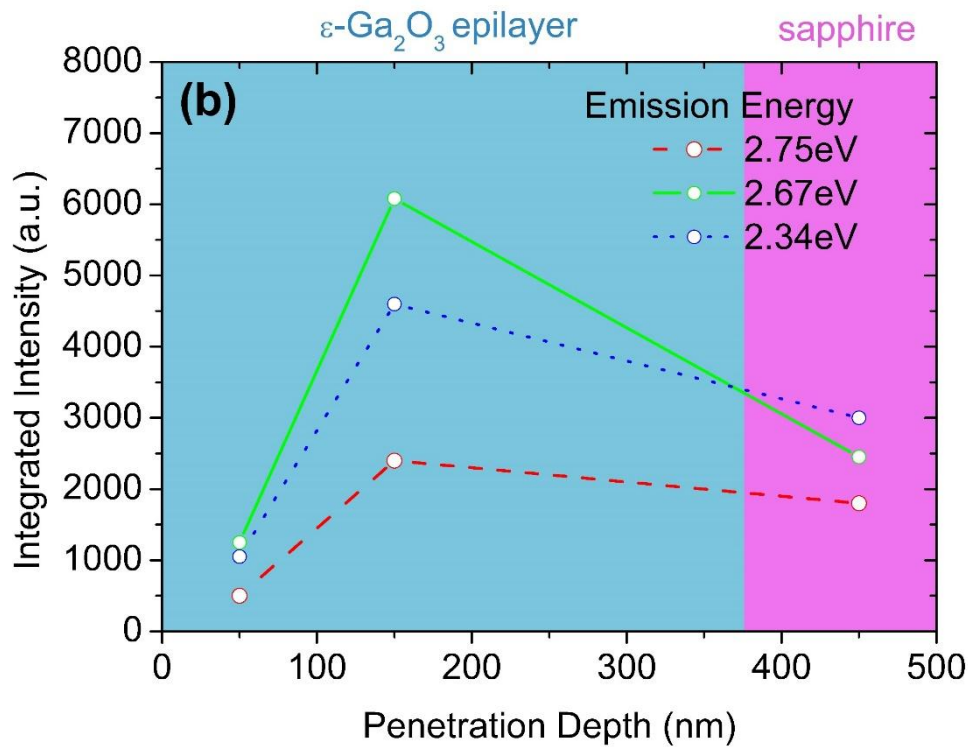
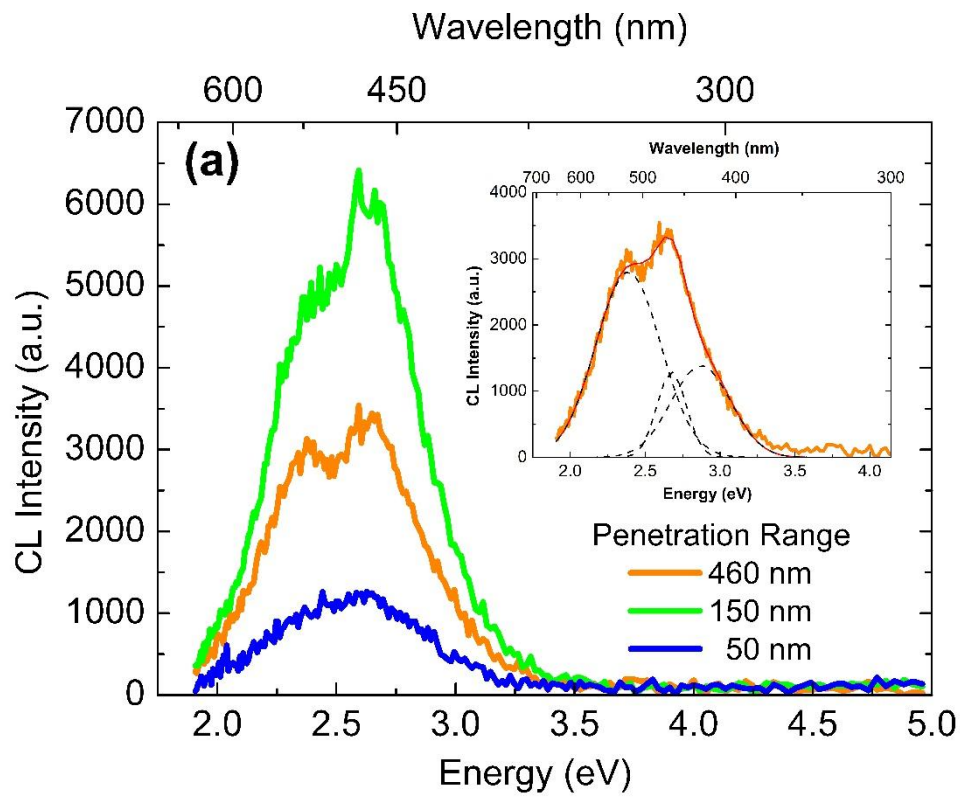


**Fig. 6:** **a)** Depth-resolved CL analysis at fixed injection power ( $10^{-5}$  W) for three different electron penetration ranges. Inset: gaussian deconvolution of the 10 keV CL spectrum; **b)** Integrated CL intensity as function of the electron penetration depth in a 380 nm thick.

1 Fig. 6b reports the integrated intensity of the three individual emission bands as function of the  
2 electron penetration depth for the same sample of Fig. 6a. The maximum intensity of the three  
3 bands always occurs corresponding to acceleration voltages of 5 kV (penetration depth of about 150  
4 nm), that means in the middle of the epilayers, away from surface and interface. The lower CL  
5 emission close to the external surface is likely related to higher density of non-radiative defects with  
6 respect to the bulk of the films. At 10 keV acceleration voltage, the generation-recombination  
7 volume surely included the interface with sapphire, and part of the substrate, so that a direct  
8 comparison with the emission intensity at lower acceleration voltages is not possible. However, it  
9 can reasonably be argued that the concentration of non-radiative defects must be higher than in the  
10 central portion of the epilayer.  
11  
12  
13  
14  
15  
16  
17  
18  
19  
20  
21

22 The physical picture provided by the different measurements is rather complicated, however it is  
23 possible to reconcile all results considering a band diagram like the one reported in Fig. 7.  
24  
25

26 Actually, the deep donor at about 0.7 eV below conduction band should be the dominant defect, in  
27 order to pin the Fermi level and to account for the experimental thermal activation energy of dark  
28 current. On the other hand, the three levels (most probably families of levels) with energies ranging  
29 from 2.3 to 2.75 eV below the conduction band may well account for the CL emission, for the  
30 pronounced absorption tail, and the weaker increase of photo-conductivity for photons of energy  
31 higher than 3.0 eV. In this model, we reasonably assumed a negligible contribution of holes to the  
32 photocurrent, due to their very low mobility. It should also be noted that the schematic bandgap of  
33 Fig 7 does not include the non-radiative deep levels. Actually, the results presented in Fig. 6b may  
34 be interpreted in two ways: either considering a maximum concentration of the radiative levels at  
35 2.3-2.75 eV in the middle of the layer section, or a minimum concentration of non-radiative killer  
36 centers in the same region of the sample. The present data do not allow removing this ambiguity,  
37 neither to clarify the role that radiative and non-radiative deep levels play in terms of the  
38 photocurrent relaxation following light switch-off. This interesting question will be certainly  
39 addressed in the near future.  
40  
41  
42  
43  
44  
45  
46  
47  
48  
49  
50  
51  
52  
53  
54  
55  
56  
57  
58  
59  
60  
61  
62  
63  
64  
65

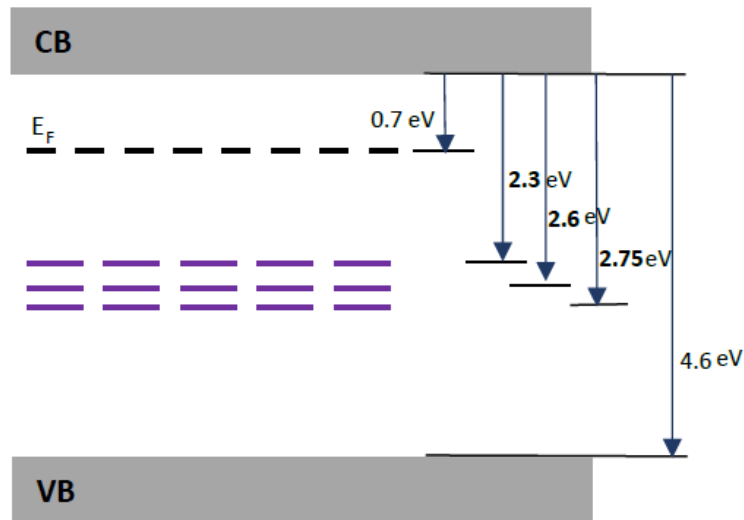


**Fig. 7:** schematic band diagram for  $\epsilon$ -Ga<sub>2</sub>O<sub>3</sub> thin films.

### 3. Conclusions

In summary, undoped single-phase  $\epsilon$ -Ga<sub>2</sub>O<sub>3</sub> epitaxial films prepared by MOCVD were investigated by photoconductivity, optical absorption and cathodoluminescence. It was observed that this “unusual” gallium oxide polymorph possesses very high dark-resistivity and a bandgap of 4.6-4.7 eV, i.e. comparable with that of  $\beta$ -Ga<sub>2</sub>O<sub>3</sub>, thus allowing the design and fabrication of solar-blind UV photodetectors. Simple photoresistors, fabricated by alloying ohmic contacts on the epilayers grown on insulating sapphire substrates, exhibited a three orders of magnitude photocurrent difference upon below/above bandgap illumination and relatively fast on/off switching times. The CL measurements revealed a broad blue emission peaked at about 2.6 eV, whose intensity changed along the film cross-section and was maximum away from surface and substrate interface. The band was deconvoluted into three narrower bands, very probably connected with native deep levels. The full set of experimental results may be explained by a band diagram including a deep donor located at 0.7 eV below the conduction band, responsible for the thermal activation of the dark current, and three deeper levels that account for the CL radiative emission and the tails of the absorption and PC spectra. Such levels (and possibly other non-radiative levels) are probably related to the transients

1 following the light on/off of the  $\epsilon$ -Ga<sub>2</sub>O<sub>3</sub> based photodetector. The physical properties and the  
2 photo-response of  $\epsilon$ -Ga<sub>2</sub>O<sub>3</sub> make this particular phase very interesting in view of novel applications.  
3  
4  
5

## 6 **Acknowledgements**

7  
8  
9 The PhD grant of F.B. was supported by Fondazione Cariparma.  
10  
11  
12  
13  
14  
15

## 16 **References**

- 17  
18  
19 [1] K. Sasaki, M. Higashiwaki, A. Kuramata, T. Masui, S. Yamakoshi, MBE grown Ga<sub>2</sub>O<sub>3</sub> and its  
20 power device applications, *J. Cryst. Growth* 378 (2013) 591-595.  
21  
22 [2] T.-C. Wei, D.-S. Tsai, P. Ravadgar, Jr-J. Ke, M.-L. Tsai, D.-H. Lien, C.-Y. Huang, R.-H. Horng,  
23 Jr-H. He, See-through Ga<sub>2</sub>O<sub>3</sub> solar-blind photodetectors for use in harsh environments, *IEEE J. Sel.*  
24 *Topics in Quant. Electr.* 20 (2014) 3802006.  
25  
26 [3] A. Kuramata, A.K. Koshi, K., S.Watanabe, Y. Yamaoka, T. Masui, S. Yamakoshi, High-quality  
27  $\beta$ -Ga<sub>2</sub>O<sub>3</sub> single crystals grown by edge-defined film-fed growth, *Japan. J. Appl. Phys.* 55, (2016)  
28 1202A2.  
29  
30 [4] P. Ravadgar, R.-H. Horng, S.-D. Yao, H.-Y. Lee, B.-R. Wu, S.-L. Ou, L.-W. Tu, Effects of  
31 crystallinity and point defects on optoelectronic applications of  $\beta$ -Ga<sub>2</sub>O<sub>3</sub> epilayers, *Optics Express*  
32 21(21) (2013) 24599.  
33  
34 [5] R. Zou, Z. Zhang, Q. Liu, J. Hu, L. Sang, M. Liao, W. Zhang, High detectivity solar-blind high-  
35 temperature deep ultraviolet photodetector based on multi-layered (1 00) facet-oriented  $\beta$ -Ga<sub>2</sub>O<sub>3</sub>  
36 Nanobelts, *Small* 10 (9) (2014) 1848–1856.  
37  
38 [6] F. Boschi, M. Bosi, T. Berzina, E. Buffagni, C. Ferrari, R. Fornari, Hetero-epitaxy of  $\epsilon$ -Ga<sub>2</sub>O<sub>3</sub>  
39 layers by MOCVD and ALD, *J. Cryst. Growth* 443 (2016) 25-30.  
40  
41 [7] R. Roy, V.G. Hill, E.F. Osborn, Polymorphism of Ga<sub>2</sub>O<sub>3</sub> and the system Ga<sub>2</sub>O<sub>3</sub>-H<sub>2</sub>O, *J. Am.*  
42 *Chem. Soc.* 74 (1952) 719-722.  
43  
44  
45  
46  
47  
48  
49  
50  
51  
52  
53  
54  
55  
56  
57  
58  
59  
60  
61  
62  
63  
64  
65

- [8] H.Y. Playford, A.C. Hannon, E.R. Barney, R.I. Walton, Structures of uncharacterised polymorphs of gallium oxide from total neutron diffraction, *Chem. Eur. J.* 19 (2013) 2803-2813.
- [9] Y. Oshima, E.G. Víllora, Y. Matsushita, S. Yamamoto, K. Shimamura, Epitaxial growth of phase-pure  $\epsilon$ -Ga<sub>2</sub>O<sub>3</sub> by halide vapor phase epitaxy, *J. Appl. Phys.* 118 (2015) 085301.
- [10] X. Xia, Y. Chen, Q. Feng, H. Liang, P. Tao, M. Xu, G. Du, Hexagonal phase-pure wide band gap  $\epsilon$ -Ga<sub>2</sub>O<sub>3</sub> films grown on 6H-SiC substrates by metal organic chemical vapor deposition, *Appl. Phys. Lett.* 108 (2016) 202103
- [11] I. Cora, F. Mezzadri, F. Boschi, M. Bosi, M. Caplovicova, G. Calestani, I. Dódony, B. Pécz, R. Fornari: “Real structure of  $\epsilon$ -Ga<sub>2</sub>O<sub>3</sub> and its relation to  $\kappa$  phase”, *Cryst. Eng. Comm.* 19 (2017) 1509
- [12] K. Irmscher, Z. Galazka, M. Pietsch, R. Uecker, R. Fornari, Electrical properties of  $\beta$ -Ga<sub>2</sub>O<sub>3</sub> single crystals grown by the Czochralski method, *J. Appl. Phys.* 110 (2011) 063720.
- [13] Z. Liu, X. Jing, L. Wang, Effects of O<sub>2</sub> partial pressure and Ga atmosphere on the luminescence of native defects in  $\beta$ -Ga<sub>2</sub>O<sub>3</sub> Phosphor, *J. Electrochem. Soc.* 154 (2007) H440-H443.
- [14] Z. Zhang, E. Farzana, A. Arehart, S.A. Ringel, Deep level defects throughout the bandgap of (010)  $\beta$ -Ga<sub>2</sub>O<sub>3</sub> detected by optically and thermally stimulated defect spectroscopy, *Appl. Phys. Lett.* 108 (2016) 052105
- [15] M. Beaudoin, M. Meunier, C.J. Arsenault, Blueshift of the optical band gap: Implications for the quantum confinement effect in a-Si:H/a-SiN<sub>x</sub>:H multilayers, *Phys. Rev. B* 47 (1993) 2197-2202.
- [16] F. Ricci, F. Boschi, A. Baraldi, A. Filippetti, M. Higashiwaki, A. Kuramata, V. Fiorentini, R. Fornari, Theoretical and experimental investigation of optical absorption anisotropy in  $\beta$ -Ga<sub>2</sub>O<sub>3</sub>, *J. Phys.: Cond. Matter* 28 (2016) 224005.
- [17] S. Rafique, Lu Han, H. Zhao, Synthesis of wide bandgap Ga<sub>2</sub>O<sub>3</sub> (E<sub>g</sub>~4.6-4.7 eV) thin films on sapphire by low-pressure chemical vapor deposition, *Phys. Stat. Sol. A* 213 (2016) 1002-1009.
- [18] D. Guo, Z. Wu, P. Li, Y. An, H. Liu, X. Guo, H. Yan, G. Wang, C. Sun, L. Li, W. Tang, Fabrication of  $\beta$ -Ga<sub>2</sub>O<sub>3</sub> thin films and solar-blind photodetectors by laser MBE technology, *Optical Mater. Exp.* 4 (2014) 1067-1076.

- 1  
2  
3  
4  
5  
6  
7  
8  
9  
10  
11  
12  
13  
14  
15  
16  
17  
18  
19  
20  
21  
22  
23  
24  
25  
26  
27  
28  
29  
30  
31  
32  
33  
34  
35  
36  
37  
38  
39  
40  
41  
42  
43  
44  
45  
46  
47  
48  
49  
50  
51  
52  
53  
54  
55  
56  
57  
58  
59  
60  
61  
62  
63  
64  
65
- [19] X.Z. Liu, P. Guo, T. Sheng, L.X. Qian, W.L. Zhang, Y.R. Li,  $\beta$ -Ga<sub>2</sub>O<sub>3</sub> thin films on sapphire pre-seeded by homo-self-templated buffer layer for solar-blind UV photodetector, *Optical Mater.* 51 (2016) 203-207.
- [20] L. Binet, D. Gourier, Origin of the blue luminescence of  $\beta$ -Ga<sub>2</sub>O<sub>3</sub>, *J. Phys. Chem. Solids* 59 (1998) 1241-1249.
- [21] T. Onuma, S. Fujioka, T. Yamaguchi, M. Higashiwaki, K. Sasaki, T. Masui, T. Honda, Correlation between blue luminescence intensity and resistivity in  $\beta$ -Ga<sub>2</sub>O<sub>3</sub> single crystals, *Appl. Phys. Lett.* 103 (2013) 041910.
- [22] F. Fabbri, M.J. Smith, D. Recht, M.J. Aziz, S. Gradečak, G. Salviati, Depth-resolved cathodoluminescence spectroscopy of silicon supersaturated with sulfur, *Appl. Phys. Lett.* 102 (2013) 031909.
- [23] D. Drouin, A.R. Couture, D. Joly, X. Tastet, V. Aimez, R. Gauvin, CASINO V2.42: a fast and easy-to-use modeling tool for scanning electron microscopy and microanalysis users, *Scanning* 29 (2007) 92-101.